19th Brazilian Congress of Thermal Sciences and Engineering
November 06th-10th, 2022, Bento Gonçalves - RS - Brazil

# ENC-2022-0201
# FEASIBILITY ASSESSMENT OF A TES UNIT OF A CSP PLANT IN BRAZIL

**Lucas Rodrigues Neumann**
**Elisa Ishitani Melo**
**André Sá Alves Vilela**
**Igor Marques Alves**
Pontifícia Universidade Católica de Minas Gerais
Av. Dom José Gaspar, 500, Coração Eucarístico, Belo Horizonte – MG, Brasil. CEP 30535-901
neumannlucaseng@hotmail.com
elisaishitani@gmail.com
andresaalvesvilela@gmail.com
igor.marques.alves@hotmail.com

**Magdalena Walczak**
Pontificia Universidad Catolica de Chile
Av Libertador Bernardo O'Higgins 340, Santiago, Región Metropolitana, Chile
mwalczak@ing.puc.cl

**Pedro Paiva Brito**
**Cristiana Brasil Maia**
Pontifícia Universidade Católica de Minas Gerais
Av. Dom José Gaspar, 500, Coração Eucarístico, Belo Horizonte – MG, Brasil. CEP 30535-901
pbrito@pucminas.br
cristiana@pucminas.br

***Abstract.*** *The recent decades have shown an increase in the population as well as the extensive usage of fossil fuels, which contributes to environmental impacts such as the pollution and greenhouse effect. Investing in clean energy and diversification of the energy matrix not only contributes to a better solution to control environmental impacts but also helps in the development of the energy industry. Solar energy is a clean and abundant energy source and is considered a potential alternative renewable source. It can be exploited by using concentrating solar power (CSP) or photovoltaic technologies. In a CSP plant, a series of mirrors are used to reflect the sunlight into an energy concentrator which is filled with a fluid used to carry this heat to drive a turbine to produce electricity. CSP utilizes four main technological approaches where trough systems, dish systems, linear Fresnel, and tower systems are utilized. Parabolic trough and tower systems have called more attention due to the higher concentrating ratios they achieve. Due to the intermittency of solar energy, these systems cannot operate at night or with low levels of solar radiation. To overcome these limitations, the newest CSP technologies are integrated with thermal energy systems (TES) increasing its dispatchability and also making this technology more competitive. The main objective of this work is to assess the transient operation of a TES system of a CSP solar tower power plant installed in the city of Januária, Brazil. The heliostat field was defined, and based on the energy available for the heat transfer fluid, a control system was proposed to improve the design and increase the performance of the plant.*

***Keywords:*** *CSP, TES, dispatchability, solar energy.*

## 1. INTRODUCTION

Nowadays, the use of renewable energy is essential to decrease both the consumption of fossil resources and the production of carbon dioxide partly responsible for the greenhouse gas effect (Ervin, 1977; International Energy Agency (IEA), 2013). There are five major renewable energy sources: solar energy from the sun, geothermal energy from the heat inside the earth, wind energy, biomass from plants, and hydropower from flowing water. Solar energy stands out as a green, low-cost, and abundant source, being widely recognized as one of the most competitive alternatives among all the

renewables (Islam *et al.*, 2018). Electricity from solar energy is usually provided by photovoltaic (PV) and concentrated solar power (CSP) technologies. CSPs use mirrors and lenses to concentrate a large area of naturally available solar energy onto a small area. The concentrated energy can be used to generate the electric power once it is converted into heat through a thermodynamic cycle (Khan and Arsalan, 2016). A CSP plant is composed of four main elements: a concentrator, a high-temperature solar receiver, a fluid transport system, and a power generation block (e.g., Rankine cycle, Brayton cycle, Stirling cycle). It is estimated by IEA that the CSP will contribute up to 11% of the global electricity production in 2050 (Power, 2010). Concentrated solar power is particularly attractive due to its advantages in terms of high efficiency, low operating cost, dispatchability, and good scale-up potential (Desideri and Campana, 2014; Zhang et al., 2013).

Four different kinds of CSP generation plants are found: solar parabolic dishes, parabolic trough collectors (PTC), solar power towers (SPT), and linear Fresnel reflectors. SPT provides greater efficiency resulting from their higher working temperatures, as well as the possibility of operating with very large capacity thermal storage systems. For these reasons, most of the recent solar power system plants and deployments have been developed with SPTs (Alonso-Montesinos *et al.*, 2019). The receivers of SPT operate at a high temperature using a heat transfer fluid, usually molten salt due to its thermal stability. A power plant integrated with a solar system usually incorporates a storage medium to leverage the potential of prolonged energy storage opportunities. Such a plant is based on its high-capacity factor achievable, low energy storage cost, higher efficiency of the integrated thermodynamic cycle, and firm output capability (Behar, Khellaf and Mohammedi, 2013; International Renewable Energy Agency (IRENA), 2013).

However, solar energy has the limitation of intermittency, which leads to fossil backup systems. This drawback is tackled by using energy storage systems in the solar plants, with thermal energy storage (TES) one of the most promising technologies (Linares *et al.*, 2020). TES can be considered a key aspect for CSP plants, as they provide not only dispatchable electricity but also stability to the electricity in case of a high fraction of renewable production or intermittency due to weather conditions. Nowadays, the two-tank systems using molten salt configuration is the most used within CSP plants (Torras *et al.*, 2015).

The solar tower power (STP) plant with thermal energy storage (TES) is considered a very promising alternative to electricity generation systems. An appropriate size of heliostat field and TES for the STP system is desired to lower the capital cost and increase the annual income from electricity generation (Sharma *et al.*, 2016). For a specific solar tower power with a TES system, optimal sizing of heliostat field and TES necessarily involves deciding the most suitable design, direct normal irradiance (DNI), and TES hours.

The main objective of this work is to evaluate a CSP plant operating with a solar tower and a $sCO_2$ Brayton cycle. The plant was simulated for Januaria, Brazil, considering a net output of 100 MW. The number of heliostats and their position were designed to ensure a heat transfer for the power block of 200 MW. The TES system was designed to minimize heat losses for the environment. A transient analysis was performed to evaluate the variation of the molten salt temperature during three days.

## 2. MATERIALS AND METHODS

The basic layout of the CSP plant studied is shown in Figure 1. The system consists of a heliostats field, a solar receiver, a TES system operating with molten salt, and a Brayton cycle operating with supercritical $CO_2$. The heliostats reflect and concentrate the solar energy onto the solar receiver. A two-tank molten salt storage system is implemented: one as the cold tank and the other as the hot one. The molten salt is pumped between both tanks for charging and discharging, while the heat is stored in the liquid salt mixture (Palacios *et al.*, 2020). The cold salt tank is heated until a given temperature (state b) in the receiver. Part of the molten salt from the hot salt tank is used to transfer energy to the $CO_2$ in the power block (thermodynamic cycle), while the remaining hot salt is stored in the hot tank. The molten salt leaving the heat exchangers is pumped to the concentrator (Solar receiver) or stored in the cold tank. When the molten salt from the receiver is not hot enough to heat the $CO_2$, the molten salt from the hot tank is used.

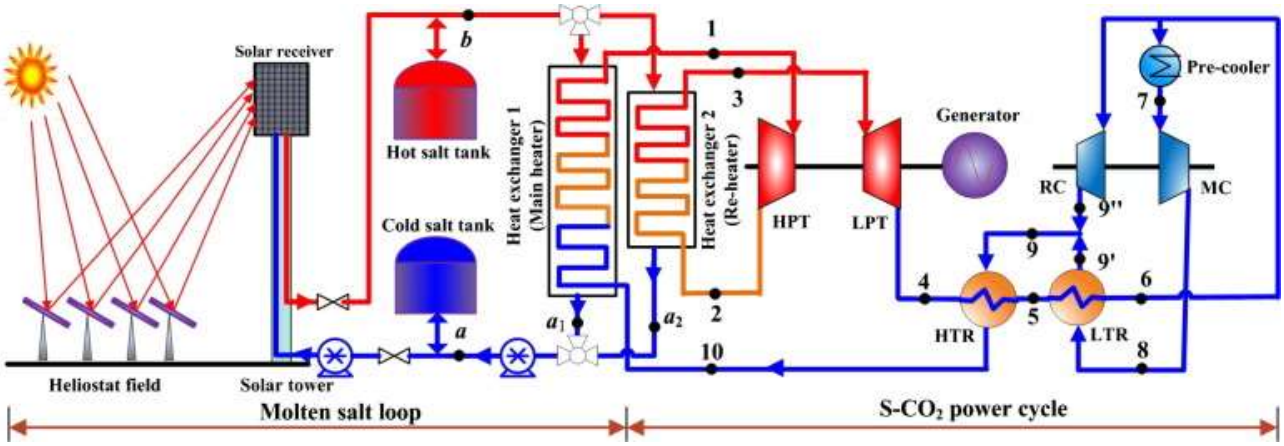

Figure 1 – Schematic diagram of the CSP plant (Wang and He, 2017)

The first step is to define the city to install the plant. Potential locations are generally identified by the distribution of Direct Normal Irradiance (DNI). Commercially viable plants should have DNI between 2000 and 2800 kWh/m$^2$, but a value higher than 1800 kWh/m$^2$ is suitable for the development of CSP plants (Islam *et al.*, 2018). Januária and Itacarambi, both located in the state of Minas Gerais, receive DNI of 1800 to 2300 kWh/m$^2$. The city of Januária was chosen by its DNI and by its location, close to the São Francisco River. It is located in the north of the state of Minas Gerais (latitude 15°29'44" S and longitude 44°21'45" W), which is located in the south-east of Brazil, as indicated in Figure 2.

Figure 2 – Location of Januária

The second step was the definition of the power output of the Brayton cycle. Based on commercial plants around the world, it was defined a net power output of 100 MW. A thermodynamic analysis of the Brayton cycle indicated that 156 MW is required in the heat exchangers, following the model suggested by (Al-Sulaiman and Atif, 2015; Linares *et al.*, 2020), (Moisseytsev and Sienicki, 2009), with fixed values for isentropic efficiencies of the compressor and turbine, and for the effectiveness of the heat exchangers. To ensure a minimum of 156 MW, the heliostats were designed to produce 200 MW. The heliostats field was designed using the SolarPilot software version 1.4. This software is provided and developed by the National Renewable Energy Laboratory (NREL) and it has been used as a tool to create a suitable field setup for solar tower applications, as shown in (Wagner and Wendelin, 2018; Yang, Yang and Duan, 2021).

The third step was the design of the TES system. The TES should be designed in such to avoid salt freezing and significant heat losses to the environment (Torras *et al.*, 2015). In this paper, a mathematical model of the governing heat transfer mechanisms is applied to determine the transient heat losses and temperatures of the molten salt. It is important to ensure that the temperature variations are not significant.

Finally, for the designed TES system, it is proposed a control system to ensure steady-state conditions on the power block, even with variations in the solar irradiance and ambient temperatures.

### 2.1 Heliostat field design

Solar tower plants, also known as central receiver systems, have complex optical properties due to the number of mirrors with individual tracking systems reflecting sunlight onto a stationary receiver throughout the day and throughout the year. The angular acceptance window for the images reflected by the heliostats is very small as it requires tracking accuracies with a standard deviation distribution error on the order of 1 mrad or less [19]. Furthermore, the receiver operation requires that the flux density is kept below a certain maximum value and that the images reflected by the heliostats are strategically reflected to achieve this distribution (Zavoico, 2001), which consequently increases the useful life of the receiver material and reduces optical losses. The redirection of sunlight by the field of heliostats is also subject to a series of losses due to the positions of the mirrors to the receiver, the positions and orientations of neighboring heliostats, atmospheric factors, and geometry of the heliostats, optical errors and the strategy operation itself in the field.

Many of the characteristic losses of the heliostat field are dynamic and therefore the field must be modeled under a series of conditions to achieve satisfactory performances in a concentrated solar power plant, which contributed to the use of software to generate the field geometry and characterize its performance since the late 1970s (Leary and Hankins, 1979; Lipps and Vant-Hull, 1978; Walzel et al., 1977). Several programs have been developed for the analysis and optimization of the solar plant as a whole or just the field of heliostats. Examples of such software are HFLCAL (to create and optimize heliostat fields), DELSOL3 (to calculate performance and perform collector modeling in the field, also optimize system design), CAMPO (field and collector design), SolTrace (to model systems and analyze their

performance), SAM (models CSP systems and calculates financial metrics), and SolarPilot (generates and characterizes tower systems). SolarPilot software version 1.4.0 was used in this paper.

The meteorological data from Januária are not in the database of SolarPilot, but the software allows to obtain irradiance data and other specific properties through the satellites provided by NREL. The user should then define some plant design variables such as the desired power in the field, as well as properties of the tower and concentrator that directly influence the number of mirrors required in the field. The main parameters are shown in Tab. 1. Other aspects, such as the optical height (h op) of the tower, which represents the height where the concentrator is located, and the type of distribution of the heliostats, were assumed as the ones suggested by the software.

Table 1. Heliostat field configuration

| **Initial parameters for heliostat field configuration** | |
|---|---|
| Solar field design power | 200 MWt |
| Design-point DNI value | 950 W/m² |

SolarPilot performs daily analysis for a specific period, so to perform the first simulation the last radiation database was used (2020), with the first day of summer and the time where the DNI was closest to the one used for the point design template. The values considered for this simulation can be seen in Tab. 2.

Table 2. Input values for a heliostat field performance simulation

| **Reference period for a performance simulation** | |
|---|---|
| Date | 12/21/2020 |
| Hour | 11:00 |
| DNI | 904 W/m² |

## 2.2 Thermal Energy Storage

Zaversky et al. (2013) proposed a mathematical model of the transient heat losses of a molten salt thermal energy storage with two tanks, differentiating from previous classical models such as the mathematical model for energy storage for the CSP plant CESA I (Castro et al., 1991). Dimensions and constructive parameters were defined for the hot and cold tanks, based on the literature, and this model was used as a reference to determine the temperature variation over three days.

The tanks are insulated on the top, laterals, and bottom, and are placed over a concrete layer over the soil. The heat transfer mechanisms considered are shown in Figure 3. The first mechanism is the convective heat transfer between the molten salt inventory and the tank's inner steel surfaces. The second mechanism is the radiative heat exchange between the molten salt surface and the non-wetted parts of the tank's inner steel jacket, divided into the molten salt surface, the tank's inner roof surface of circular planar shapes, and the tank's non-wetted inner wall surface of cylindrical shape. The third mechanism is the heat exchange between the tank's outer surface and the ambient, by radiation and convection, which is subdivided into natural and forced convection. The radiative heat transfer at the tank's outer surface considers both the absorbed solar irradiation (on the roof and the outer wall) and the emitted long wave radiation to the ambient. The last mechanism is the bottom heat loss of the tank, divided into the conductive heat losses from the concrete foundation into the soil, and the convective heat losses from the concrete foundation to the ambient air.

This model was applied both to the hot salt tank and to the cold salt tank. The temperature defined for the hot tank was 560°C since molten salts degrade above 565°C (Achkari and El Fadar, 2020). The temperature defined for the cold tank was 290°C, above the freezing point. The main reason for storing the salt at both temperatures is to keep the highest temperature delta while still avoiding freezing and degradation issues due to its thermal stability and high crystallization temperature (Sau *et al.*, 2016).

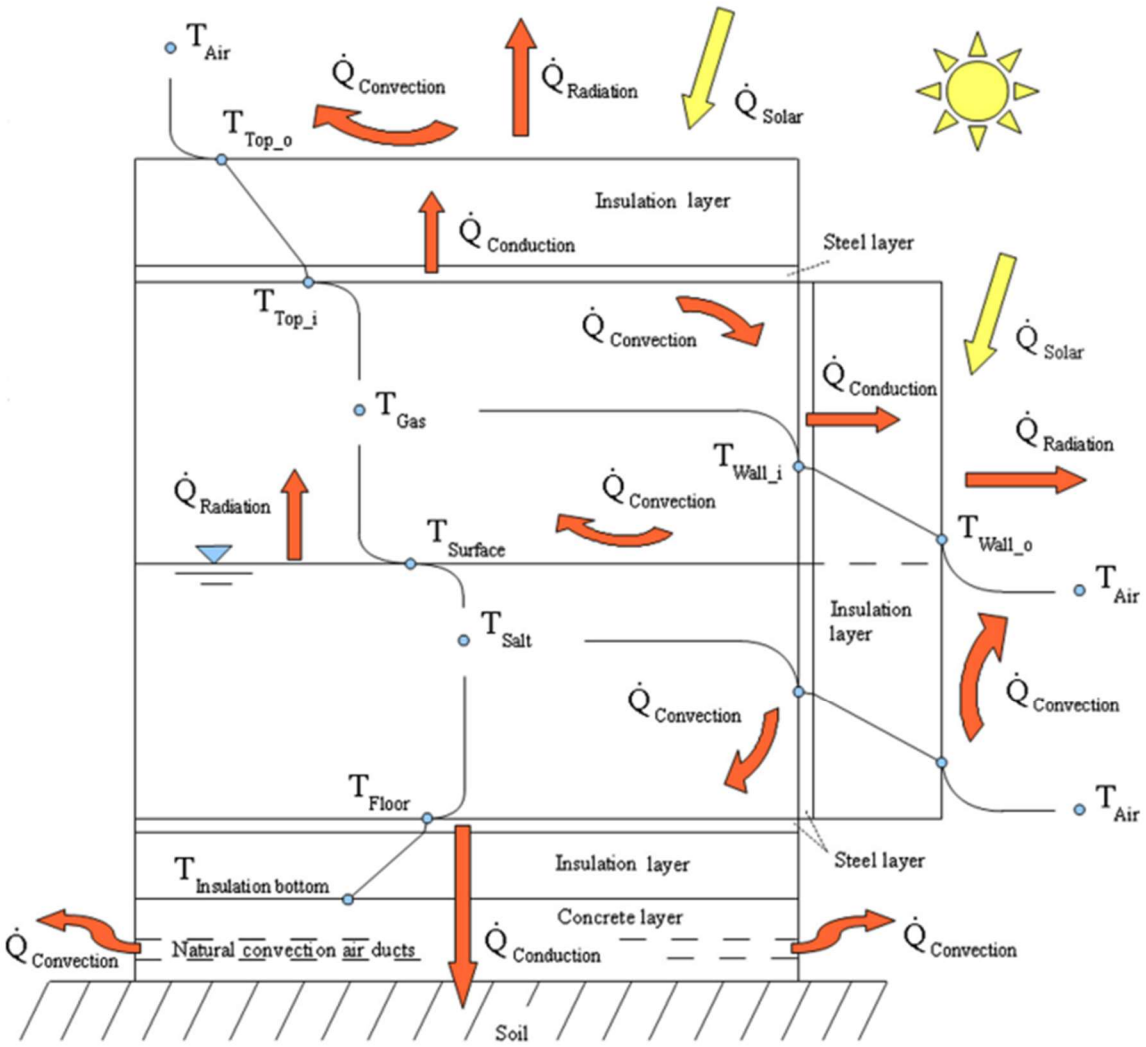


Figure 3. Molten salt thermal storage tank model scheme – temperature e distributions and heat flows. *(Zaversky* et al.*, 2013)*

The model analysis can be carried out in terms of mass-energy balance for the correspondent control volume in terms of mass flow rate $\dot{m}$, enthalpy h, and heat flux $\dot{Q}_{liq}$ (Zaversky *et al.*, 2013).

$$\frac{dm}{dt} = \dot{m}_{in} - \dot{m}_{out} \quad (1)$$

$$U = m.u \quad (2)$$

$$\frac{dU}{dt} = \dot{m}_{in} . h_{in} - \dot{m}_{out} . h_{out} + \dot{Q}_{liq} \quad (3)$$

Where $\dot{m}$ is the mass in the control volume, $\dot{m}_{in}$ and $\dot{m}_{out}$ are the inlet and outlet mass flow, $h_{in}$ and $h_{out}$ are the specific enthalpies at the inlet and outlet of the control volume, U is the total internal energy and u is the specific internal energy of the control volume. For the analysis of heat transfer, the molten salt is assumed as an incompressible liquid with the properties suggested by Ferri et al. (2008)

The transient analysis has been carried out for three days, considering charging, and discharging periods.

### 2.3 Control System

The solar energy input is transient, but the thermodynamic cycle must operate under steady-state conditions. A control system is required to provide dispatchable power on demand at any time of the day (Palacios *et al.*, 2020), allowing the conversion of thermal energy into electrical energy uninterruptedly as a function of the cycle demand.

The operation of the TES is divided into three processes: charging, discharging, and stand-by.

During storage system charging mode, the molten salt is pumped from the cold tank and fed into the hot tank, while passing through a heat exchanger, where the molten salt reaches the hot tank temperature level. The discharging process occurs by pumping the molten salt from the hot tank through the heat exchanger to the cold tank while transferring the required heat from the molten salt (Zaversky *et al.*, 2013). During the stand-by, the thermal storage system acts as a secondary source, feeding the main line of the cycle when the molten salt that circulates does not have enough thermal energy to feed the power cycle. It is defined as an initial condition that the temperature variation is not higher than $T_{max} - T_{min}$.

## 3. RESULTS

The city of Januária was defined as the location for the installation of the plant. The yearly distribution of the maximum direct solar irradiation is shown in Figure 4. Although the maximum DNI for November reaches 1027 W/m², the value of 950W/m$^2$ was used as a design-point point for the heliostat field simulation.

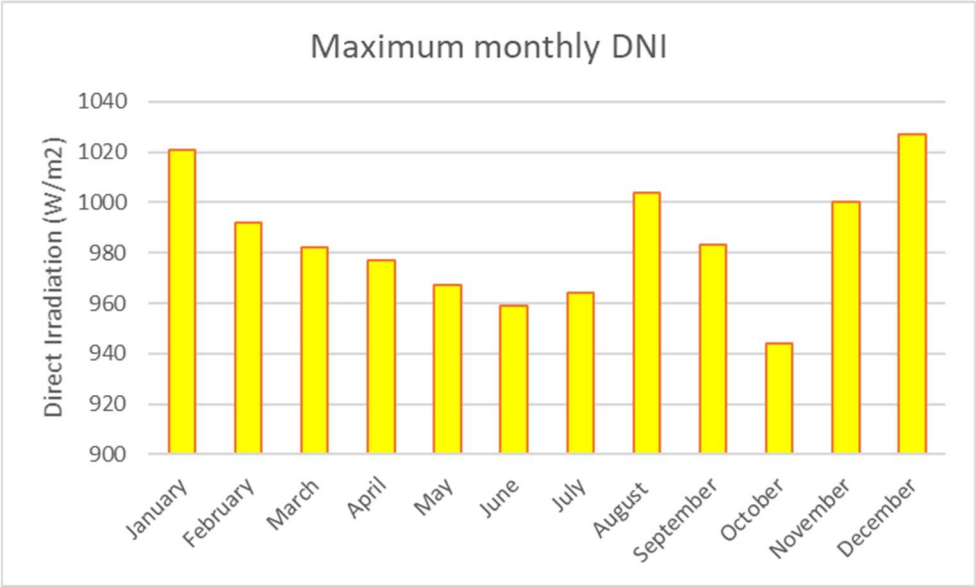


Figure 4. Maximum Monthly Irradiation for Januária in 2020 ((NREL, 2022))

Using the SolarPilot software for the production of 200 MW, as previously discussed, an area of heliostats of 380716 m$^2$ is required, with the configuration shown in Figure 5. The colors represent the efficiency of the individual heliostats, which varied from 54.0 to 86.2% on 20 December at 11:00. The main characteristics of the heliostat field are shown in Table 3.

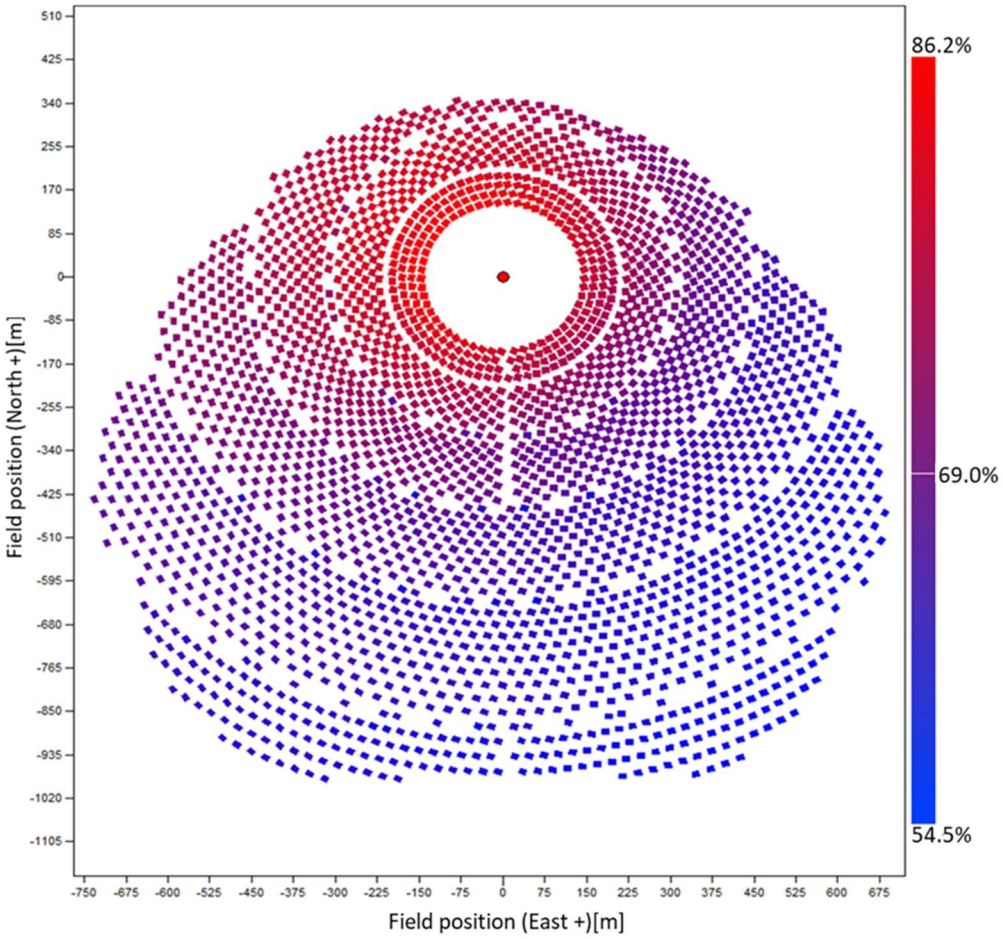


Figure 5. Heliostat Field configuration

Table 3. Simulated field results

| Field specifications | Units | Value |
|---|---|---|
| Simulated heliostat area | m² | 380716 |
| Simulated heliostat count | - | 2637 |
| Power incident on the field | kW | 344168 |
| Power absorbed by the receiver | kW | 223170 |
| Power absorbed by HTF | kW | 185250 |
| Image intercept efficiency | % | 99.11 |
| Absorption efficiency | % | 94.00 |
| Solar field optical efficiency | % | 68.98 |
| Optical efficiency incl. receiver | % | 64.84 |
| Annualized heliostat efficiency | % | 0.00 |
| Incident flux | kW/m² | 198.23 |

The dimensions of the tanks were defined based on the literature (Zaversky *et al.*, 2013), and the main geometric and constructive parameters are shown in Table 4.

Table 4. Hot and cold tank parameters

| Parameters | Hot Tank | Cold Tank |
|---|---|---|
| Height | 14 m | 14 m |
| Diameter | 38.5 m | 38.5 m |
| Insulating materials | Mineral wool, calcium silicate board, foam glass | Mineral wool, calcium silicate board, foam glass |
| Insulating thickness | 0.4 m | 0.3 m |
| Wall thickness | 0.04 m | 0.04 m |
| Tank Material | Stainless Steel 304 Cr-Ni (18-20%) | Stainless Steel 304 Cr-Ni (18-20%) |

The mathematical model was simulated for 3 days. Figure 6 shows the distribution of the molten salt surface temperature over time. It can be seen that the temperature variation has reached less than 1°C for both hot and cold tanks either full or empty. When comparing the temperature inside the tanks (290 and 560°C), it is observed that this temperature drop can be neglected, indicating that the tank design is suitable.


Figure 6. Temperature variation of the molten salt for Hot and Cold tanks

To ensure that the power block will operate under steady-state conditions, it is required a heat transfer of 165 MW in the heat exchanger of the thermodynamic cycle at any time. The checking point is the comparison of the temperatures of the molten salt and the maximum achievable temperature. The mass flow rate is then adjusted to ensure the required heat, according to

$$\dot{Q} = \dot{m} \, . \, c_p \, . \, \Delta T \qquad (4)$$

The temperature variation should not exceed $T_{max} - T_{min}$.

Table 5 exemplifies the control parameters for the mass flow rate. During charging mode, the molten salt is pumped from the cold tank to the hot tank, passing through the receiver. If the molten salt temperature is lower than the maximum temperature, the mass flow rate is kept constant and the molten salt is kept on the receiver until its temperature reaches the maximum temperature. Auxiliary reheaters are off. Once the maximum temperature is reached, the mass flow rate increases to fill the hot tank during the specified charging time and also feed the thermodynamic cycle with the required thermal potency. Once stand-by starts, the thermodynamic cycle is fed by the molten salt in the line while the receptors keep this salt temperature at the maximum value. During this process, the salt in the hot tank remains stored. If the temperature of the salt in the line is not high enough for the thermodynamic cycle, part of the salt stored in the hot is mixed in the line, the heaters are turned on, and the mass flow rate increases. The discharging mode starts once the radiation is over. The cycle now is powered by the molten salt that is being released from the hot tank, and the molten salt that was previously in the line is now pumped to the cold tank. The heaters remain turned on and the mass flow increases to ensure the power required to run the cycle.

Table 3. Control parameters for mass flow rate

| Mode | Molten salt temperature in the Receptor ($T_{salt}$) | Action TES Hot/ Cold | Action Receptor | Action Pump | Action re-heaters |
|---|---|---|---|---|---|
| **Charging** | $T_{salt}<T_{max}$ | None/ pump to the Concentrator | Heat until $T_{salt} = T_{max}$ | Keep Mass Flow rate | Off |
| | $T_{salt} = T_{max}$ | Fill/pump to the thermodynamic cycle | Heat until $T_{salt} = T_{max}$ | Increase Mass Flow rate | Off |
| **Stand-by** | $T_{salt} = T_{max}$ | None/ None | Heat until $T_{salt} = T_{max}$ | Keep Mass Flow rate | Off |
| | $T_{salt} \leq T_{max}$ | Release Moten Salt as per demand/ None | Heat until $T_{salt} \cong T_{max}$ | Increase Mass Flow rate | On |
| **Discharging** | Closed Valve | Discharge/ Charge | None | Increase Mass Flow rate | On |

## 4. CONCLUSIONS

In this paper, an analysis of a CSP solar tower power plant with TES has been conducted for the city of Januária - MG. The plant was designed to produce a net power of 100 MW in a $sCO_s$ Brayton cycle. It was defined the configuration of the heliostats field for the first day of the summer, for 11:00. The design point of the heliostat field has been set as 200 MW. The simulation showed that 380716 square meters of heliostats are required, operating with efficiencies ranging between 54.0 and 86.2%. An energy balance showed that the temperature drop throughout the day is negligible, and the design of the hot and cold tanks is suitable to avoid thermal losses to the ambient. Finally, the proposed control system ensures the required heat is delivered to the power cycle at any time.

## 5. ACKNOWLEDGMENTS

The authors are thankful to the PUC Minas, FAPEMIG, and CNPq. This study was financing in part by the Coordenação de Aperfeiçoamento de Pessoal de Nível Superior - Brasil (CAPES) - Finance Code 001.

## 6. REFERENCES

Achkari, O. and El Fadar, A. (2020) “Latest developments on TES and CSP technologies – Energy and environmental issues, applications and research trends,” *Applied Thermal Engineering* [Preprint]. https://doi.org/10.1016/j.applthermaleng.2019.114806.

Alonso-Montesinos, J. *et al.* (2019) “Impact of DNI forecasting on CSP tower plant power production,” *Renewable Energy*, 138. https://doi.org/10.1016/j.renene.2019.01.095.

Al-Sulaiman, F.A. and Atif, M. (2015) "Performance comparison of different supercritical carbon dioxide Brayton cycles integrated with a solar power tower," *Energy*, 82. https://doi.org/10.1016/j.energy.2014.12.070.

Behar, O., Khellaf, A. and Mohammedi, K. (2013) "A review of studies on central receiver solar thermal power plants," *Renewable and Sustainable Energy Reviews*. https://doi.org/10.1016/j.rser.2013.02.017.

Castro, M. *et al.* (1991) "C.R.S. receiver and storage systems evaluation," *Solar Energy*, 47(3). https://doi.org/10.1016/0038-092X(91)90079-C.

Desideri, U. and Campana, P.E. (2014) "Analysis and comparison between a concentrating solar and a photovoltaic power plant," *Applied Energy*, 113. https://doi.org/10.1016/j.apenergy.2013.07.046.

Ervin, G. (1977) "Solar heat storage using chemical reactions," *Journal of Solid State Chemistry*, 22(1). https://doi.org/10.1016/0022-4596(77)90188-8.

Ferri, R., Cammi, A. and Mazzei, D. (2008) "Molten salt mixture properties in RELAP5 code for thermodynamic solar applications," *International Journal of Thermal Sciences*, 47(12). https://doi.org/10.1016/j.ijthermalsci.2008.01.007.

International Energy Agency (IEA) (2013) "World Energy Outlook 2013 Paris:OECD/IEA," *International Energy Agency* [Preprint].

International Renewable Energy Agency (IRENA) (2013) "Renewable power generation costs in 2012: An Overview," *Irena* [Preprint].

Islam, M.T. *et al.* (2018) "A comprehensive review of state-of-the-art concentrating solar power (CSP) technologies: Current status and research trends," *Renewable and Sustainable Energy Reviews* [Preprint]. https://doi.org/10.1016/j.rser.2018.04.097.

Khan, J. and Arsalan, M.H. (2016) "Solar power technologies for sustainable electricity generation - A review," *Renewable and Sustainable Energy Reviews* [Preprint]. https://doi.org/10.1016/j.rser.2015.10.135.

Leary, P.L. and Hankins, J.D. (1979) *User's guide for MIRVAL: a computer code for comparing designs of heliostat-receiver optics for central receiver solar power plants*, *Sand-77-8280*.

Linares, J.I. *et al.* (2020) "A novel supercritical CO2 recompression Brayton power cycle for power tower concentrating solar plants," *Applied Energy*, 263. https://doi.org/10.1016/j.apenergy.2020.114644.

Lipps, F.W. and Vant-Hull, L.L. (1978) "A cellwise method for the optimization of large central receiver systems," *Solar Energy*, 20(6). https://doi.org/10.1016/0038-092X(78)90067-1.

Moisseytsev, A. and Sienicki, J.J. (2009) "Investigation of alternative layouts for the supercritical carbon dioxide Brayton cycle for a sodium-cooled fast reactor," *Nuclear Engineering and Design*, 239(7). https://doi.org/10.1016/j.nucengdes.2009.03.017.

NREL (2022) *National Solar Radiation Database Data Viewer*. Available at: https://maps.nrel.gov/nsrdb-viewer (Accessed: June 18, 2022).

Palacios, A. *et al.* (2020) "Thermal energy storage technologies for concentrated solar power – A review from a materials perspective," *Renewable Energy* [Preprint]. https://doi.org/10.1016/j.renene.2019.10.127.

Power, C.S. (2010) "Technology Roadmap Concentrating Solar Power," *Current*, 5.

Sau, S. *et al.* (2016) "Techno-economic comparison between CSP plants presenting two different heat transfer fluids," *Applied Energy*, 168. https://doi.org/10.1016/j.apenergy.2016.01.066.

Sharma, C. *et al.* (2016) "A study of the effect of design parameters on the performance of linear solar concentrator based thermal power plants in India," *Renewable Energy*, 87. https://doi.org/10.1016/j.renene.2015.11.007.

Torras, S. *et al.* (2015) "Parametric Study of Two-tank TES Systems for CSP Plants," in *Energy Procedia*. https://doi.org/10.1016/j.egypro.2015.03.206.

Wagner, M.J. and Wendelin, T. (2018) "SolarPILOT: A power tower solar field layout and characterization tool," *Solar Energy*, 171. https://doi.org/10.1016/j.solener.2018.06.063.

Walzel, M.D., Lipps, F.W. and Vant-Hull, L.L. (1977) "A solar flux density calculation for a solar tower concentrator using a two-dimensional hermite function expansion," *Solar Energy*, 19(3). https://doi.org/10.1016/0038-092X(77)90067-6.

Wang, K. and He, Y.L. (2017) "Thermodynamic analysis and optimization of a molten salt solar power tower integrated with a recompression supercritical CO2 Brayton cycle based on integrated modeling," *Energy Conversion and Management*, 135. https://doi.org/10.1016/j.enconman.2016.12.085.

Yang, J., Yang, Z. and Duan, Y. (2021) "Load matching and techno-economic analysis of CSP plant with S–CO2 Brayton cycle in CSP-PV-wind hybrid system," *Energy*, 223. https://doi.org/10.1016/j.energy.2021.120016.

Zaversky, F. *et al.* (2013) "Transient molten salt two-tank thermal storage modeling for CSP performance simulations," *Solar Energy*, 93. https://doi.org/10.1016/j.solener.2013.02.034.

Zavoico, A.B. (2001) "Solar Power Tower - Design Basis Document," *Technical Report SAND2001-2100* [Preprint], (July). https://doi.org/10.2172/786629.

Zhang, H.L. *et al.* (2013) "Concentrated solar power plants: Review and design methodology," *Renewable and Sustainable Energy Reviews*. https://doi.org/10.1016/j.rser.2013.01.032.